DMD Fast Forward. Published on June 24, 2020 as DOI: 10.1124/dmd.119.090092
This article has not been copyedited and formatted. The final version may differ from this version.

Title Page

Abemaciclib Does Not Have a Clinically Meaningful Effect on Pharmacokinetics of CYP1A2, CYP2C9, CYP2D6, and CYP3A4 Substrates in Patients with Cancer

P. Kellie Turner, Stephen D. Hall, Sonya C. Chapman, Jessica Rehmel,

Jane Royalty, Yingying Guo, Palaniappan Kulanthaivel

Eli Lilly and Company, Indianapolis, IN (PKT, SDH, SCC, YG, PK);

Covance Early Clinical Development, Madison, WI (JR)

DMD Fast Forward. Published on June 24, 2020 as DOI: 10.1124/dmd.119.090092
This article has not been copyedited and formatted. The final version may differ from this version.

The study was sponsored by Eli Lilly and Company.

DMD Fast Forward. Published on June 24, 2020 as DOI: 10.1124/dmd.119.090092
This article has not been copyedited and formatted. The final version may differ from this version.

Running Title Page:

Running title: Effect of abemaciclib on CYP1A2, 2C9, 2D6 and 3A4 substrates

Corresponding author:
P. Kellie Turner
Eli Lilly and Company
Lilly Corporate Center
Indianapolis, IN 46285
317-651-8361
turnerpa@lilly.com

Manuscript word count:
Abstract: 238
Intro: 428
Discussion: 1017

List of Non-standard Abbreviations:

AhR, aryl hydrocarbon receptor; $AUC_{0\text{-}24}$, area under the concentration versus time curve from zero to 24 hours; $AUC_{0\text{-}inf}$, area under the concentration versus time curve from zero to infinity; AUCR, area under the concentration versus time curve ratio; CAR, constitutively active receptor; CDK4, cyclin dependent kinase 4; CDK6, cyclin dependent kinase 6; C_{max}, maximal observed plasma concentration; CT, cycle threshold; CTCAE, Common Terminology Criteria for Adverse Events; CYP, cytochrome P450; EC_{50}, half maximal response concentration; DDI, drug-drug interaction; ECOG, Eastern Cooperative Oncology Group; EMA, European Medicines Agency; E_{max}, maximum extent of induction or downregulation; F_a, fraction of drug absorbed; F_g, fraction of drug escaping metabolism in the gut; f_m, fraction of systemic clearance; $f_{u.p}$, fraction of drug unbound in plasma; GAPDH, glyceraldehyde 3-phosphate dehydrogenase; INR, international normalized ratio; INR $AUC_{(0\text{-}96)}$, area under the international normalized ratio versus time curve from time zero to 96 hours post-dose; k_a, absorption rate constant; LC/MS, liquid chromatography/mass spectrometry; LDH, lactate dehydrogenase; M2, N-desethylabemaciclib; M20, hydroxyabemaciclib; MMAE, monomethyl auristatin E; MR, metabolic ratio; PD, pharmacodynamics; PK, pharmacokinetics; PM, poor metabolizer; PXR, pregnane X receptor; Q_h, hepatic blood flow; Q12H, every 12 hours; Q_{en}, enterocyte blood flow; R_b, blood-to-plasma ratio; RT-qPCR, reverse transcription quantitative polymerase chain reaction; TEAE, treatment-emergent adverse event; $t_{1/2}$, half-life; t_{max}, time of maximum observed drug concentration.

DMD Fast Forward. Published on June 24, 2020 as DOI: 10.1124/dmd.119.090092
This article has not been copyedited and formatted. The final version may differ from this version.

Abstract:

Abemaciclib is an orally administered, potent inhibitor of cyclin dependent kinases 4 and 6 (CDK4 and CDK6) and is metabolized extensively by cytochrome P450 (CYP) 3A4. The effects of abemaciclib on several CYPs were qualified *in vitro* and subsequently evaluated in a clinical study. *In vitro*, human hepatocytes were treated with vehicle, abemaciclib, or abemaciclib metabolites (M2 or M20). mRNA levels for 8 CYPs were measured using RT-qPCR and, additionally, catalytic activities for 3 CYPs were determined. In the clinical study, adult cancer patients received a drug cocktail containing CYP substrates (midazolam [3A], warfarin [2C9], dextromethorphan [2D6], and caffeine [1A2]) either alone or in combination with abemaciclib. Plasma PK samples were analyzed for all substrates, caffeine metabolite paraxanthine, and abemaciclib; polymorphisms of CYP2C9, CYP2D6, CYP3A4, and CYP3A5 were evaluated. *In vitro*, downregulation of CYP mRNA, including 1A2, 2B6, 2C8, 2C9, 2D6, and 3A, by abemaciclib and/or M2 and M20 was observed at clinically relevant concentrations. In humans, abemaciclib did not affect the PK of CYP2D6 or CYP2C9 substrates, and minor statistically significant but clinically irrelevant changes were observed for midazolam ($AUC_{0\text{-}inf}$ [13% lower] and C_{max} [15% lower]), and caffeine ($AUC_{0\text{-}inf}$ [56% higher]) and paraxanthine: caffeine ($AUC_{0\text{-}24}$ ratio [was approximately 30% lower]). However, given the magnitude of the effect, these changes are not considered clinically relevant. In conclusion, the downregulation of CYP mRNA mediated by abemaciclib *in vitro* did not translate into clinically meaningful drug-drug interactions in cancer patients.

DMD Fast Forward. Published on June 24, 2020 as DOI: 10.1124/dmd.119.090092
This article has not been copyedited and formatted. The final version may differ from this version.

Significance Statement

Despite observations that abemaciclib alters the mRNA of various CYP isoforms *in vitro*, a clinical study using a drug cocktail approach found no clinically meaningful drug-drug interactions between abemaciclib and a range of CYP substrates (midazolam [CYP3A4], S-warfarin [CYP2C9], dextromethorphan [CYP2D6], and caffeine [CYP1A2]). This lack of translation suggests greater understanding of mechanisms of CYP downregulation is needed to accurately predict clinical DDI risk from *in vitro* data.

DMD Fast Forward. Published on June 24, 2020 as DOI: 10.1124/dmd.119.090092
This article has not been copyedited and formatted. The final version may differ from this version.

Introduction:

Abemaciclib is an orally administered, selective cyclin-dependent kinase-4 (CDK4) and CDK6 inhibitor approved for the treatment of hormone receptor positive (HR+), human epidermal growth factor receptor 2 negative (HER2-) advanced or metastatic breast cancer (Dickler MN et al., 2016). Abemaciclib is primarily metabolized by cytochrome P450 (CYP) 3A4, producing 2 major (>10% circulating exposure) equipotent metabolites, M2 (LSN2839567 [N-desethylabemaciclib]) and M20 (LSN3106726 (hydroxyabemaciclib).

Given that abemaciclib is dependent on CYP3A4 for elimination, 2 clinical drug-drug interaction (DDI) studies were performed to assess the impact of CYP3A induction and inhibition on the exposure of abemaciclib and its active metabolites. Rifampin, a strong CYP3A inducer, decreased the area under the concentration versus time curve (AUC) of abemaciclib by 95% (Kulanthaivel P et al., 2016). Following dosing with clarithromycin, a strong CYP3A inhibitor, the AUC ratio for abemaciclib was 3.4 (Kulanthaivel P et al., 2016; Posada MM, et al., 2017). Accordingly, labeling includes recommendations around the concomitant use of CYP3A inducers and inhibitors (Eli Lilly and Company, 2017; European Medicines agency, 2012). While the effect of other drugs on abemaciclib is well characterized, the effects of abemaciclib on the pharmacokinetics of CYP substrate drugs has not been extensively explored.

The incubation of drug and major metabolites with cultured human hepatocytes provides a convenient and efficient approach to assess whether significant CYP induction or downregulation of CYP expression occurs *in vitro*. The mechanisms responsible for CYP induction have been described in detail (Sun Y et al., 2017) and the induction response of CYP3A4 mRNA in hepatocytes translates into the clinic (Fahmi OA et al., 2010). In contrast, although *in vitro* CYP downregulation *in vitro* has been described (Hariparsad N et al., 2017), the generalizability of the mechanisms is unknown and clinical translation has not been verified. Thus, the detection of CYP downregulation *in vitro* is generally followed by a clinical drug

DMD Fast Forward. Published on June 24, 2020 as DOI: 10.1124/dmd.119.090092
This article has not been copyedited and formatted. The final version may differ from this version.

interaction study requiring multiple doses of the putative inhibitor. This is to allow the target enzymes to approach a new steady state which is estimated to be 7 days based on CYP degradation half-lives of 24 to 36 hours (Yang J et al., 2008)

In the present study, we evaluated the effects of abemaciclib and its major active metabolites, M2 and M20, on CYP1A2, CYP2B6, CYP2C8, CYP2C9, CYP2C19, CYP2D6, and CYP3A4 and CYP3A5 mRNA expression in cultured human hepatocytes. Based on the *in vitro* results, we conducted a clinical study in cancer patients to assess the effects of multiple doses of abemaciclib on the PK of a cocktail of CYP substrates, namely midazolam (CYP3A4), S-warfarin (CYP2C9), dextromethorphan (CYP2D6), and caffeine (CYP1A2).

Materials & Methods:

In Vitro Studies

Abemaciclib, M2, and M20 were supplied by Eli Lilly and Company (Indianapolis, IN). Cryopreserved primary human hepatocytes and supplemented Modified Eagle Medium (with Dr. Chee's modification; MCM+) were obtained from XenoTech LLC (Lenexa, KS), with lot-specific details given in **Supplemental Table 1**. Phenacetin, acetaminophen, bupropion hydrochloride, midazolam, omeprazole, phenobarbital, and rifampicin were obtained from Sigma Aldrich (St. Louis, MO). Hydroxybupropion and 1'-hydroxymidazolam were from Cerilliant (Round Rock, TX). Stable-label internal standards for acetaminophen, hydroxybupropion, and 1'-hydroxymidazolam were from a proprietary source. Reagents for RNA isolation and PCR were from Applied Biosystems and Qiagen.

Primary human hepatocytes in culture were treated with vehicle, abemaciclib, or M2, or M20 for 48 hours. Abemaciclib was incubated with a single lot of cells while M2 and M20 were each incubated with 3 lots of cells. Quantitative evaluation of cytotoxicity was measured using a lactate dehydrogenase (LDH) release assay (Roche Diagnostics, Indianapolis, IN). mRNA levels for CYP1A2, CYP2B6, CYP2C8, CYP2C9, CYP2C19, CYP2D6, CYP3A4, and CYP3A5,

DMD Fast Forward. Published on June 24, 2020 as DOI: 10.1124/dmd.119.090092
This article has not been copyedited and formatted. The final version may differ from this version.

as well as the endogenous control, glyceraldehyde 3-phosphate dehydrogenase (GAPDH), were measured using RT-qPCR with specific assays listed in **Supplemental Table 2.** Catalytic activities for CYP1A2, CYP2B6, and CYP3A4 were measured using selective catalytic assays for CYP1A2 (phenacetin O-deethylation to acetaminophen), CYP2B6 (bupropion hydroxylation), and CYP3A4 (midazolam 1'-hydroxylation) as described in **Supplemental Table 3**. Omeprazole (50 μM) served as the positive control for aryl hydrocarbon receptor (AhR)-mediated induction of CYP1A2, phenobarbital (750 μM) was the positive control for constitutively active receptor (CAR)-mediated induction of CYP2B6, and rifampicin (20 μM) was the positive control for pregnane X receptor (PXR)-mediated induction of the remaining inducible CYPs. Data are reported for non-cytotoxic concentrations as determined by LDH release, increases in cycle threshold (CT) values for GAPDH, and/or morphological observations. Criteria for induction were concentration-dependent increases in mRNA expression of greater than or equal to 2-fold and a response greater than or equal to 20% of the positive control response. Concentration-dependent decreases in mRNA of greater than or equal to 50% were considered downregulation.

To model the effect of downregulation of CYP3A4 on the oral clearance of midazolam, non-linear regression using a 4-parameter logistic model was used to estimate E_{max}, the maximum extent of induction or downregulation, and EC_{50}, the half maximal response concentration (Graphpad Prism version 7, San Diego, CA). The E_{max} and EC_{50} for CYP3A4 were entered in a simplified mechanistic static net effect model (Equation 1)(Fahmi OA et al., 2008) to predict the AUCR (ratio of AUC with and without downregulation) for orally administered midazolam.

Equation 1. $$AUCR = \frac{1}{\left(1-\frac{Emax\times[I]g}{[I]g+EC_{50}}\right)\times(1-F_g)+F_g} \times \frac{1}{\left(1-\frac{Emax\times[I]_h}{[I]_h+EC_{50}}\right)\times f_m+1-f_m}$$

DMD Fast Forward. Published on June 24, 2020 as DOI: 10.1124/dmd.119.090092
This article has not been copyedited and formatted. The final version may differ from this version.

Where f_m is the fraction of systemic clearance of midazolam via CYP3A4 (set at 0.9), F_g is the fraction of midazolam escaping metabolism in the gut (set at 0.5), $[I]_H$ is the concentration of perpetrator drug at the liver (Equation 2), and $[I]_G$ is the concentration of perpetrator drug at the intestine (Equation 3), with inputs as shown in **Supplemental Table 4**.

Equation 2. (Ito K et al., 1998). $[I]_h = f_{u,p} \times (C_{max} + F_a \times k_a \times Dose/Q_h/R_b)$

Equation 3. (Rostami-Hodjegan A et al., 2004). $[I]_g = F_a \times k_a \times Dose/Q_{en}$

Clinical Study Design

This Phase 1, multicenter, open-label, fixed-sequence study (NCT02688088) was conducted in patients with advanced and/or metastatic cancer. The enrolled patients were at least 18 years of age with an Eastern Cooperative Oncology Group (ECOG) score between 0 and 2 and adequate organ function. The study excluded patients who had surgery performed that could affect the absorption or experience emesis which may affect drug PK.

The study was conducted in accordance with ethical principles derived from international ethics guidelines, including the Declaration of Helsinki, and Council for International Organizations of Medical Sciences (CIOMS) International Ethical Guidelines, the ICH GCP guideline, and applicable laws and regulations.

Treatment. A drug cocktail containing 4 sensitive CYP substrates was selected based on a subset of the validated Cooperstown 5+1 cocktail, namely midazolam (CYP3A4), S-warfarin (CYP2C9), dextromethorphan (CYP2D6), and caffeine (CYP1A2) (Chainuvati S et al., 2003). A CYP2B6 substrate was not included due to the low number of drugs dependent on CYP2B6 clearance. The cocktail containing 0.2 mg midazolam, 10 mg warfarin, 30 mg dextromethorphan, and 100 mg caffeine was administered orally as a single dose on 2 occasions: alone on Day 1 in Period 1, and in combination with abemaciclib on Day 8 of Period 2. Abemaciclib was administered continuously at 200 mg Q12H for 7 days prior to drug cocktail

DMD Fast Forward. Published on June 24, 2020 as DOI: 10.1124/dmd.119.090092
This article has not been copyedited and formatted. The final version may differ from this version.

administration in order for abemaciclib steady state concentrations to be reached (Patanaik A et al., 2016) and for any time-dependent changes in CYP activity to take full effect (~3-5 CYP half-lives (36 hours) (**Fig. 1. Study Design**). Abemaciclib dose interruptions or modifications were avoided where possible but were permitted if needed due to individual intolerability. Food consumption was not permitted 1 hour before or after taking abemaciclib or the drug cocktail. Known inducers and/or inhibitors of CYP1A2, CYP2C9, CYP2D6, and CYP3A4 were excluded 14 days prior to drug cocktail administration and throughout Periods 1 and 2; participants were also asked to refrain from consuming grapefruit juice, Seville oranges, and St. John's Wort during the same timeframe. Dietary caffeine consumption was not permitted 5 days prior to drug cocktail administration and throughout Periods 1 and 2. In patients reporting treatment-emergent adverse events (TEAEs), the abemaciclib dose was lowered from 200 mg twice daily to 150 mg twice daily. If the patient had an international normalized ratio (INR) of more than 2 after the first dose of drug cocktail, abemaciclib was only dosed thereafter once the INR had returned to acceptable levels. If patients had an INR greater than 2 in Period 1, they may have received the drug cocktail without warfarin in Period 2.

Evaluation Methods

Assays. Human plasma samples were analyzed for abemaciclib, M2, M20, and midazolam (Q2 Solutions; Ithaca, NY, USA), as well as S-warfarin, dextromethorphan, caffeine, and paraxanthine (Covance Bioanalytical Services, LLC; Indianapolis, IN, USA) using validated liquid chromatography with tandem mass spectrometric (LC/MS/MS) methods.

Pharmacokinetics. PK samples were collected on Period 1 Day 1 and Period 2 Day 8 pre-dose, and 0.5, 1, 2, 3, 4, 6, 8, 12, and 24 hours post-dose for caffeine, paraxanthine and midazolam, with an additional sample at 48 hours for midazolam. PK samples for dextromethorphan and S-warfarin were collected at pre-dose and 1, 2, 4, 6, 8, 10, 24, 48, and

DMD Fast Forward. Published on June 24, 2020 as DOI: 10.1124/dmd.119.090092
This article has not been copyedited and formatted. The final version may differ from this version.

72 hours post-dose on Day 1 (Period 1) and Day 8 (Period 2), with an additional sample at 96 hours for S-warfarin. Pre-dose PK samples were taken in Period 2 on Days 7-9 for abemaciclib.

Pharmacodynamics. Blood samples were collected pre-dose, and 8, 24, 48, 72, and 96 hours post-dose on Period 1, Day 1 and Period 2, Day 8 to assess INR AUC_{0-96} and INR_{max}.

Pharmacogenomics. A blood sample for each patient was collected in vacutainer EDTA tubes either during the baseline visit or pre-dose (Period 1, Day 1). Genomic DNA was then extracted for *CYP2C9, CYP2D6, CYP3A4*, and *CYP3A5*, and genotyping was performed by validated TaqMan® qPCR assays (Thermo Fisher Scientific, Waltham, MA) and long-range PCR assays (Fijal BA et al., 2015) at Covance Genomics Laboratory (Redmond, WA). These included alleles of *CYP2D6*2, *3, *4, *5, *6, *7, *8, *9, *10, *17, *29, *41*, and duplications, *CYP2C9*2*, and **3, CYP3A4*3, *7, *20*, and **22*, as well as *CYP3A5*3, *4, *5, *6*, and **7*. The functional-determining genetic variant for each star allele was selected and assayed according to the Human Cytochrome P450 (CYP) Allele Nomenclature Database. Allele frequencies were tested for Hardy-Weinberg equilibrium within each ethnic group and considered significant at $p<.0001$. Patients were classified into metabolizer groups for each CYP based on the combination of alleles associated with their genotype (Birdwell KA et al., 2019; Hicks JK et al., 2017; Ingelman-Sundberg M et al., 2007; Johnson JA et al., 2011). Patients who were poor metabolizers for any CYP were evaluated for exclusion from the DDI statistical analysis of the respective probe substrate.

Statistical Methods

Pharmacokinetic and Pharmacodynamic endpoints. Midazolam, S-warfarin, dextromethorphan, caffeine, and paraxanthine PK (e.g., C_{max}, AUC_{0-inf}, and t_{max}) and S-warfarin PD ($INRAUC_{(0-96)}$ or INR_{max}) were calculated by standard noncompartmental methods (Phoenix WinNonlin Version 6.4). The ratio between paraxanthine and caffeine exposure was calculated for the 6-hour concentration timepoint and for AUC_{0-24}. Log-transformed C_{max} and AUC_{0-inf}

DMD Fast Forward. Published on June 24, 2020 as DOI: 10.1124/dmd.119.090092
This article has not been copyedited and formatted. The final version may differ from this version.

estimates were evaluated in a linear mixed-effects analysis of variance model with a fixed effect for treatment and a random effect for subject. The treatment differences were back-transformed to present the ratio of geometric least squares means and the corresponding 90% confidence intervals (CIs). The t_{max} was analyzed using a Wilcoxon signed rank test. Estimates of the median difference based on the observed medians, 90% CIs, and p-values from the Wilcoxon test were calculated.

Safety. Adverse event terms and severity grades were assigned by the investigator using Common Terminology Criteria for Adverse Events (CTCAE, Version 4.0).

Results:

In vitro Studies

First, the effect of abemaciclib and metabolites on catalytic activity of CYP enzymes was assessed. In human liver microsomes, abemaciclib and its major circulating metabolites, M2 and M20, did not inhibit the catalytic activities of CYP1A2, CYP2B6, CYP2C8, CYP2C9, CYP2C19, CYP2D6, or CYP3A4 either directly or in a time-dependent manner at clinically relevant circulating concentrations for abemaciclib (0.59 µM), M2 (0.27 µM), and M20 (0.38 µM). No reversible or time-dependent inhibition of CYPs was expected in the liver based on the *in vitro* data from human liver microsomes for abemaciclib, M2, or M20. However, due to poor solubility concentrations achieved *in vitro* were not sufficiently high (12.5 µM for abemaciclib) to rule out CYP3A4 inhibition at the intestine (relevant concentration 0.1*dose/250 mL = 160 µM) (European Medicines agency 2012).

We next assessed the effect of abemaciclib and metabolites on mRNA expression. Downregulation of CYP mRNA, including 1A2, 2B6, 2C8, 2C9, 2D6, 3A4, and 3A5 (but not 2C19), by abemaciclib and/or M2 and M20 was observed in the *in vitro* study conducted in human hepatocytes **(Fig. 2 panels A, B, and C)**. This mRNA downregulation was concentration dependent, greater than 50%, and not due to cytotoxicity to cells according to evaluation of 3

DMD Fast Forward. Published on June 24, 2020 as DOI: 10.1124/dmd.119.090092
This article has not been copyedited and formatted. The final version may differ from this version.

endpoints. Furthermore, in studies in human hepatocytes, abemaciclib and metabolites did not induce the catalytic activities of CYP1A2, CYP2B6, or CYP3A4. Instead, activity for all 3 CYPs decreased; CYP3A4 activity shown as an example in **Figure 2D** (Eli Lilly and Company, 2017). An overall tabular summary of the interpretation of the data for abemaciclib, M2, and M20, including selected E_{max} and EC_{50} values, is shown in **Supplemental Table 1**, and the mean data, presented as % change from 0.1% DMSO (vehicle) control is shown in **Supplemental Table 5**.

In the case of CYP2D6, both induction (up to 2.87-fold change) and marked decreases (up to 79.3%) in mRNA levels were observed when hepatocytes were treated with abemaciclib across the concentration range **(Supplemental Table 1; Fig. 2)**. For CYP3A4 mRNA, E_{max} and EC_{50} based on fitting of the data for abemaciclib were -0.89-fold and 0.37 µM, respectively. Application of the mechanistic static model (Equation 1) predicted an AUCR of 2.0 for oral midazolam due to CYP3A4 downregulation by abemaciclib. When M2 and M20 were included in the calculation (affecting midazolam model systemic clearance only) the AUCR increased to 2.1.

Clinical trial

Demographics and disposition. The majority of the 44 patients enrolled in the study were Caucasian (91%) with a mean age of 60 years (range: 37 to 78 years)(**Table 1**). Most patients had an ECOG status of 0 (27.3%) or 1 (68.2%).

Of the 44 patients who entered the study and received at least 1 dose of study drug, 37 completed Period 2. There were 2 patients who discontinued prior to Day 1 of Period 2, 1 due to fatal disease progression, and 1 due to a TEAE of increased bilirubin.

Pharmacokinetics. Up to 44 patients were included in the PK analysis for Period 1 and up to 37 were included in Period 2. The PK profiles for each analyte in the presence and absence of abemaciclib are shown in **Figure 3.** Individual changes in $AUC_{0\text{-}24}$ are shown in **Figure 4**.

DMD Fast Forward. Published on June 24, 2020 as DOI: 10.1124/dmd.119.090092
This article has not been copyedited and formatted. The final version may differ from this version.

Midazolam. The midazolam $AUC_{0\text{-}inf}$ was approximately 13% lower and the C_{max} was approximately 15% lower when midazolam was administered after multiple doses of abemaciclib versus when midazolam was administered alone with no significant differences in median t_{max}. The lower bound of the 90% CI for the ratios for midazolam $AUC_{0\text{-}inf}$ and C_{max} were below 0.8 (0.775 and 0.760, respectively)(

S-warfarin. No significant differences in the geometric least squares (LS) mean S-warfarin C_{max}, $AUC_{0\text{-}inf}$ or t_{max} between warfarin administered alone or in combination with abemaciclib were evident (**Table 2; Fig. 5**). There were also no significant differences in $INR_{AUC(0\text{-}96)}$ or INR_{max} when warfarin was administered after multiple doses of abemaciclib (geometric mean [CV%], 1.27 [34%], 1.56 [44%], respectively) compared to when administered alone (120 [23%] and 1.43 [32%], respectively).

Dextromethorphan. Based on the CYP2D6 genotyping results, 70.5% of patients were extensive metabolizers, 9.1% were intermediate metabolizers, 2.3% were ultra-rapid metabolizers, 2.3% were poor metabolizers (PM), and in 9.1% the genotype could not be interpreted. Data from the patient with PM status was excluded from the statistical analysis for dextromethorphan; however, those with unknown status were included in the analysis. Abemaciclib had no statistically significant effects on dextromethorphan C_{max}, $AUC_{0\text{-}inf}$ or t_{max} (**Table 2; Fig. 5)**.

Caffeine/paraxanthine. The AUC0-inf of caffeine was 56.0% higher when caffeine was administered after multiple abemaciclib doses compared to administration alone, with the upper limit of the 90% CI for the ratio of geometric LS mean exceeding the 1.25 boundary; however, there were no significant differences in caffeine C_{max} or t_{max} (**Table 2; Fig. 5**). The ratio between paraxanthine and caffeine (P:C) decreased by 38.9% at the P:C 6-hour time point and decreased by 31.7% for P:C $AUC_{0\text{-}24}$ in the presence of abemaciclib **(Table 2)**.

Non-compliance with caffeine restriction was evident in the data, both before and after drug cocktail administration, as demonstrated by higher than expected levels of caffeine in

DMD Fast Forward. Published on June 24, 2020 as DOI: 10.1124/dmd.119.090092
This article has not been copyedited and formatted. The final version may differ from this version.

pre-dose samples and in samples taken after the patient had left the clinical research unit (24 and 48 hours postdose)(**Supplemental Fig. 1**). Quantifiable predose caffeine concentrations of more than 10% of C_{max} were observed in Period 1 (n=4) and Period 2 (n=5), and 2 patients exhibited post-CRU increases in caffeine concentrations in both study Periods. There was 1 patient who exhibited both predose caffeine concentrations greater than 10% of C_{max} and rising concentrations after CRU discharge in both study Periods.

Abemaciclib. The geometric mean abemaciclib trough concentrations following Q12H abemaciclib oral dosing with 200 mg (the highest approved dose) or 150 mg (if the patient had experienced a dose reduction) were between 453 ng/mL (0.89 µM) and 561 ng/mL (1.11 µM)

Safety. A total of 250 TEAEs were reported, of which the majority (87.6%) were Grade 1 or Grade 2 in severity, and 11.2% of patients experienced greater than or equal to Grade 3 events. Overall, the most common drug-related TEAEs of any grade were diarrhea (56.8%), nausea (25.0%), and vomiting (25.0%). AEs greater than or equal to Grade 3 observed included 2 events of vomiting and 5 events of diarrhea. Abemaciclib-induced AEs were generally manageable and monitorable. Four patients reported serious adverse events. This included 1 patient each with CTCAE Grade 2 abdominal pain, Grade 3 diarrhea (n=1), and fractured radius (n=1) and Grade 3 cholangitis (n=1) related to other medical conditions, as well as Grade 3 ascites (n=1) which was disease-related. The only study drug related events were abdominal pain and diarrhea. One patient death was reported during Period 1 (drug cocktail in the absence of abemaciclib) due to disease progression.

Discussion:

Patients receiving abemaciclib for the treatment of cancer are likely to receive other drugs to manage their condition and/or other non-related illnesses. Many of these concomitant medications are likely to be CYP substrates. The present study investigated the potential *in vitro*

DMD Fast Forward. Published on June 24, 2020 as DOI: 10.1124/dmd.119.090092
This article has not been copyedited and formatted. The final version may differ from this version.

and clinical effect of abemaciclib and its major circulating equipotent metabolites, M2 and M20, on the exposures of other CYP substrate drugs.

During *in vitro* studies, abemaciclib-mediated concentration-dependent downregulation of several CYPs in cultured human hepatocytes was observed. The mechanism(s) underlying this observation is unknown, although the similarity of the downregulation pattern across abemaciclib, M2 and M20 suggest a common mechanism may be involved. One possible explanation could be *in vitro* metabolism of abemaciclib, M2 and M20, which results in a common downregulating species. Poor evidence exists for the translation of *in vitro* CYP downregulation to *in vivo* changes in PK. For CYP3A4, some small molecules downregulate mRNA expression in hepatocytes *in vitro* by binding to and downregulating the nuclear factor PXR, which mediates the upregulation of this enzyme by inducers (Burk O et al., 2018; Staudinger JL, 2019; Tian Y 2013). *In vivo* exploration of the clinical effects of antibody--conjugated momethyl auristatin E (MMAE, the active moiety of brentuxumab vedotin), another *in vitro* downregulator of CYP3A4 without reduced cell viability, was hindered by low systemic exposures due to antibody-conjugated MMAE delivery. This lack of effect of MMAE on the clearance of midazolam can be explained by the relevant *in vitro* concentrations not being achieved *in vivo* (Wolenski FS et al., 2018). Despite the numerous examples of CYP downregulation *in vitro*, there is no clear example of CYP *in vitro* downregulation translating into meaningful DDIs in the clinic. The possible exceptions are 1) the effect of obeticholic acid on caffeine but not its metabolite paraxanthine (Edwards JE et al., 2017) and 2) the simultaneous inhibition and down-regulation of CYP2D6 mediated by bupropion (Sager JE et al., 2017). Notably, the EMA has reviewed a clinical package for a drug which exhibited downregulation of CYP activity both *in vitro* and *in vivo* (Hariparsad N et al., 2017); however, no details of this package are publicly available at this time. Until sufficient knowledge and methodologies are

DMD Fast Forward. Published on June 24, 2020 as DOI: 10.1124/dmd.119.090092
This article has not been copyedited and formatted. The final version may differ from this version.

developed to reliably translate *in vitro* CYP downregulation into clinical DDIs predictions, any potentially concerning *in vitro* observations should be investigated further in the clinic.

For abemaciclib, which is extensively cleared by CYP3A4, clinical monotherapy PK data did not indicate any evidence of auto-inhibition (Eli Lilly and Company, 2017), suggesting abemaciclib would also not increase the exposure of the CYP3A4 substrate, midazolam. However, using the mechanistic static model with the *in vitro* down-regulation data reported herein, a 2-fold change in midazolam AUC was predicted, driven predominantly by inhibition at the gut wall. Despite these contrasting findings and general absence *in vitro-in vivo* connectivity for CYP3A inhibition due to downregulation, the clinical investigation included midazolam to evaluate the effect of abemaciclib on the PK of CYP3A substrates. Indeed, the clinical study ruled out abemaciclib-mediated CYP3A inhibition, with marginal decreases in midazolam AUC, suggesting either an inconsequential degree of abemaciclib-mediated CYP3A4 induction or reduced absorption. Similarly, Wang and colleagues report *in vitro* downregulation of CYP3A4 mRNA by carfilzomib in human hepatocytes *in vitro* which did not affect midazolam pharmacokinetics in cancer patients [$AUC_{0-\infty}$ ratio (least squares mean (90% geometric CI) 108.2 (94.1-124) (Wang Z et al., 2013). Conversely, it was shown that -weak induction of CYP3A mediated midazolam clearance by the retinoid compounds was indeed predictable based on *in vitro* studies (Stevison F et al., 2019). These studies again highlight the currently unreliable prediction of *in vivo* DDIs from *in vitro* data for CYP induction and/or down regulation. Of note, static models may overpredict drug interactions in cases of reversible inhibition and rapidly changing concentrations. However, a static model was deemed appropriate for this evaluation because 1) the down-regulation is mainly occurring at the gut where concentrations are high for a relatively short period generally coinciding with the absorption of midazolam, 2) at steady state, abemaciclib and metabolites have relatively low fluctuation between C_{max} and C_{min}, thus concentrations are not rapidly changing, and 3) changes due to down-regulation would be

DMD Fast Forward. Published on June 24, 2020 as DOI: 10.1124/dmd.119.090092
This article has not been copyedited and formatted. The final version may differ from this version.

expected to occur relatively slowly. That is, the long-enzyme turnover half-lives dampen the effect of changes in enzyme regulation.

For CYP2D6, the pathway is minimally regulated by transcription (Sager JE et al., 2017) and consequently the potential for induction is rarely studied (Hariparsad N et al., 2017). We thus expected no change in CYP2D6 mRNA levels following incubation with abemaciclib and metabolites. However, the *in vitro* data suggested mixed effects of abemaciclib on CYP2D6 induction at concentrations up to 5µM and downregulation at higher concentrations. As there was no effect of multiple doses of 200 mg abemaciclib Q12H on dextromethorphan (AUCR 0.976 [0.805, 1.18]), both the *in vitro* induction and downregulation appear to be false positives. The ability to predict *in vivo* CYP2D6 induction from *in vitro* studies is mixed: Sager et al. successfully predicted CYP2D6-mediated DDIs for bupropion based on simultaneous CYP2D6 inhibition and induction (Sager JE et al., 2017), but *in vitro* CYP2D6 downregulation by retinoids identified by Stevison et al. did not translate into the clinic (Stevison F et al., 2019).

The CYP1A2 substrate, caffeine, exhibited statistically significant increases in AUC, but the analysis was confounded by evidence of non-compliance with the dietary restriction of caffeine. For this reason, the caffeine metabolite, paraxanthine, was subsequently analyzed to determine the mechanism of any change in caffeine PK and to lessen the confounding effect of dietary caffeine consumption. The ratio of paraxanthine to caffeine (AUC or 6-hour concentrations) reflects the formation clearance of paraxanthine, the major CYP1A2 metabolite of caffeine, and has been utilized to quantify CYP1A2 activity (Tian et al., 2019). Using this approach, the present study suggests abemaciclib inhibits the CYP1A2-mediated metabolism of caffeine to paraxanthine. However, given the magnitude of intrasubject variability for caffeine AUC (34%)(data on file), the inhibitory effect of abemaciclib on CYP1A2 is not considered clinically meaningful. This study highlights the inherent challenges in using caffeine as a substrate, especially in the outpatient setting where caffeine consumption cannot be controlled.

DMD Fast Forward. Published on June 24, 2020 as DOI: 10.1124/dmd.119.090092
This article has not been copyedited and formatted. The final version may differ from this version.

Therefore, including the paraxanthine:caffeine ratio prospectively as a primary endpoint would be advised when caffeine is used as a probe substrate.

In conclusion, the downregulation of CYP mRNA expression and activity by abemaciclib *in vitro* did not translate into the clinic. No clinically relevant changes in the PK of CYP1A2, CYP2C9, CYP2D6, or CYP3A substrate drugs were observed when co-administered with multiple doses of abemaciclib. This lack of translation suggests the specific CYP mechanisms of downregulation *in vitro* need to be better understood and further work is warranted to develop appropriate models to better inform clinical DDI risk.

Acknowledgements:

The authors wish to acknowledge Jill Chappell for her expertise in study design and implementation. The study was sponsored by Eli Lilly and Company.

Authorship Contributions:

Participated in research design: Turner, Kulanthaivel, Rehmel, Royalty, Guo, Hall

Responsible for in vitro experiments: Rehmel

Performed data analysis: Chapman, Rehmel

Wrote or contributed to the writing of the manuscript: Turner, Hall, Chapman, Rehmel, Royalty, Guo, Kulanthaivel.

Disclosures

P. Kellie Turner, Stephen D. Hall, Sonya C. Chapman, Jessica Rehmel, and Yingying Guo-Avrutin are employees and minor stockholders of Eli Lilly and Company. At the time of the research, Palaniappan Kulanthaivel was an employee and minor stockholder of Eli Lilly and Company. Jane Royalty is an employee at Covance.

References:

Birdwell KA, Decker B, and Barbarino JM (2019) Clinical pharmacogenetics implementation consortium (CPIC) guidelines for CYP3A5 genotype and tacrolimus dosing. *Clin Pharmacol Ther* **98**(1):19-25.

Blanchard J and Sawers SJA (1983) The absolute bioavailability of caffeine in man. *Eur J Clin Pharmacol* **24**:93-98.

Burk O, Kuzikov M, Kronenberger T, et al (2018) Identification of approved drugs as potent inhibitors of pregnane X receptor activation with differential receptor interaction profiles. *Archives of Toxicol* **92**:1435-1451.

Chainuvati S, Nafziger AN, Leeder JS, et al (2003) Combined phenotypic assessment of cytochrome P450 1A2, 2C9, 2C19, 2D6, and 3A in N-acetyltransferase-2, and xhanthine oxidase activities with the "Cooperstown 5+1 cocktail". *Clin Pharmacol Ther* **74**(5):437-447.

Dickler MN, Tolaney SM, Rugo HS, et al (2017) MONARCH 1, a phase II study of abemaciclib, a CDK4 and CDK6 inhibitor, as a single agent, in patients with refractory HR+/HER2- metastatic breast cancer. *Clin Cancer Res* **23**(17):5218-5224.

Edwards JE: Eliot L, Parkinson A, Karan S, and MacConell L (2017) Assessment of pharmacokinetic interactions between obeticholic acid and caffeine, midazolam, warfarin, dextromethorphan, omeprazole, rosuvastatin, and digoxin in phase 1 studies in healthy subjects. *Adv Ther* **34**:2120-2138.

Eli Lilly and Company. Abemaciclib prescribing information. 2017. Available at: http://uspl.lilly.com/verzenio/verzenio.html#pi. Accessed 22-Apr-2019

European Medicines agency. Guideline on the investigation of drug interactions. 2012. Available at: https://www.ema.europa.eu/en/documents/scientific-guideline/guideline-investigation-drug-interactions_en.pdf P23 paragraph just above A:2 RIS. Accessed 22-Apr-2019.

Fahmi OA, Maurer TS, Kish M, et al (2008) A combined model for predicting CYP3A4 clinical net drug-drug interaction based on CYP2A4 inhibition, inactivation, and induction determined in vitro. *Drug Metab Disposition* **36**(8):1698-1708.

Fahmi OA, Maurer TS, Kish M, et al (2008) A combned model for predicting CYP3A4 clinical net drug-drug interaction based on CYP3A4 inhibition, inactivation, and induction determined in vitro. *Drug Metab Dispos* **36**:1698-1708.

Fahmi OA and Ripp SL (2010) Evaluation of models for predicting drug-drug interactions due to induction. *Expert Opin Drug Metab* **6**(11):1399-1416.

Fijal BA, Guo Y, Li SG, et al (2015) CYP2D6 predicted metabolizer status and safety in adult patients with attention-deficit hyperactivity disorder participating in a large placebo-controlled atomoxetine maintenance of response clinical trial. *J Clin Pharmacol* **55**(10):1167-1174.

Hariparsad N, Ramsden D, Palamanda J, et al (2017) Considerations from the IQ induction working group in response to drug-drug interaction guidances from regulatory agencies: focus on down-regulation, CYP2C induction, and CYP2B6 positive control. *Drug Metab Dispos* 10.1124/dmd.116.074567

Hicks JK, Sangkuhl K, Swen JJ, et al (2017) Clinical pharmacogenetics implementation consortium guideline (CPIC) for CYP2D6 and CYP2C19 genotypes and dosing of tricyclic antidepressants: 2016 update. *Clin Pharmacol Ther* **102**(1):37-45.

Ingelman-Sundberg M, Sim SC, Gomez A, and Rudriguez-Antona C (2007) Influence of cytochrome P450 polymorphisma of drug therapies: Pharmacogenetic, pharmacoepigenetic and clinical aspects. *Pharmacol Ther* **116**:496-526.

Ito K, Iwatsubo T, Kanamitsu S, Ueda K, Suzuki H, and Sugiyama Y (1998) Prediction of pharmacokinetic alterations caused by drug-drug interactions: metabolic interaction in the liver. *Pharmacological Rev* **50**(3):387-411.

Johnson JA, Gong L, Whirl-Carrillo M, et al (2011) Clinical pharmacogenetics implementation consortium guidelines for CYP2C9 and VKORC1 genotypes and warfarin dosing. *Clin Pharmacol Ther* **90**(4):625-630.

Kulanthaivel P, Mahadevan D, Turner PK, et al. Pharmacokinetic drug interactions between abemaciclib and CYP3A inducers and inhibitors. 107th Annual Meeting of the American Association of Cancer Research 16-20 Apr, 2016.

Patanaik A, Rosen LS, Tolaney SM, et al (2016) Efficacy and safety of abemaciclib, an inhibitor of CDK4 and CDK6, for patients with breast cancer, non-small cell lung cancer, and other solid tumours. *Cancer Discov* **6**(7):740-753.

Posada MM, Turner PK, Kulanthaivel P, Hall SD, and Dickinson GL. Predicting clinical effects of CYP3A perpetrators on abemaciclib and active metabolites exposure using physiologically-based pharmacokinetic modelling. American Society for Clinical Pharmacology and Therapeutics Annual Meeting 15-18 Mar, 2017.

Rostami-Hodjegan A and Tucker G (2004) 'In silico' simulations to assess the 'in vivo' consequences of 'in vitro' metabolic drug-drug interactions. *Drug Discov Today* **1**(4):441-449.

Sager JE, Tripathy S, Price LSL et al (2017) In vitro and in vivo extrapolation of the complex drug-drug interaction of bupropion and its metabolites with CYP2D6; simultaneous reversible inhibition of CYP2D6 downregulation. *Biochem Pharmacol* **123**:85-96.

Staudinger JL (2019). Clinical applications of small molecule inhibitors of pregnane X receptor. *Molec Cellular Endocrinol* **485**:61-71.

Stevison F, Kosaka M, Kenny JR, et al (2019) Does in vitro cytochrome P450 downregulation translate to in vivo drug-drug interactions? Preclinical and clinical studies with 13-cis-retinoic acid. *Clin Transl Sci* 10.1111.cts.12616: 1-11.

Sun Y, Chothe P, Sager JE, et al (2017) Quantitative prediction of CYP3A4 induction: impact of measured, free, and intracellcular perpetrator concentrations of human hepatocyte induction studies on drug-drug interaction predictions. *Drug Metab Dispos* **45**:692-705.

Tate SC, Sykes AK, Kulanthaivel P, Chan EM, Turner PK, and Cronier DM (2018) A populatoin pharmacokinetic and pharmacodynamic analysis of abemaciclib in a phase 1 clinical trial in cancer patients. *Clin Pharmacokinet* **57**:335-344.

Tian DD, Natesan S, White JR, and Paine MF (2019) Effects of common CYP1A2 genotypes and other key factors in individual variation in the caffeine metabolic ratio: an exploratory analysis. *Clin Transl Sci* **12**:39-46.

Tian Y (2013) Epigenetic regulation of pregnane X receptor activity. *Drug Metab Rev* **45**(2):166-172.

United States Food and Drug Administration. Clinical drug interaction studies-Study design, data analysis, and clinical implications guidance for industry. 2017. Available at: https://www.fda.gov/downloads/drugs/guidances/ucm292362.pdf. Accessed 22-Apr-2019

Wang Z, Yang J, Kirk C, et al (2013) Clinical pharmacokinetics, metabolism, and drug-drug interaction of carfilozimib. *Drug Metab Dispos* **41**:230-237.

Wolenski FS, Xia CQ, Ma B, Han TH, Shyu WC, and Balani SK (2018) CYP suppressoin in human hepatocytes by monomethyl auristatin E, the payload in brentuximab vedotin (Adcetris), is associated with microtubule disruption. *Eur J Drug Metab Pharmacokinet* **43**:347-354.

Yang J, Liao M, Shou M, et al (2008) Cytochrome P450 turnover: Regulation of synthesis and degradation, methods for determining rates, and implications for the prediction of dgu interactions. *Current Drug Metab* **9**:384-393.

DMD Fast Forward. Published on June 24, 2020 as DOI: 10.1124/dmd.119.090092
This article has not been copyedited and formatted. The final version may differ from this version.

Legends for Figures:

Figure 1. Study Design

PK, pharmacokinetics; Q12H, every 12 hours.

Figure 2. Representative Data Showing the Effects of Abemaciclib and Metabolites (M2 and M20) on CYP1A2, CYP2B6, and CYP3A4 mRNA in Human Hepatocytes incubated for 48 hours. Panel A: The effects of abemaciclib on CYP1A2 mRNA. Panel B: The mixed effects of abemaciclib on CYP2D6 mRNA. Panel C: The effects of abemaciclib (circles), M2 (x), and M20 (squares) on CYP3A4 mRNA in lot HC3-22. Panel D: The effects of abemaciclib on CYP3A4 activity. An overall tabular summary of the data for abemaciclib, M2, and M20 is shown in Supplemental Table 1, and mean data at individual concentrations is shown in Supplemental Table 5.

Figure 3. Mean Plasma Concentration-Time Profiles of Midazolam, S-Warfarin, Dextromethorphan, Caffeine, and Paraxanthine After Administration of a CYP Substrate Drug Cocktail Containing 0.2 mg Midazolam (CYP3A4), 10 mg Warfarin (CYP2C19), 30 mg Dextromethorphan (CYP2D6), and 100 mg Caffeine (CYP1A2) Either Alone (black), or In Combination with Abemaciclib After 7 Days of 200 mg Q12H Abemaciclib (red).

CYP, cytochrome P450; Q12H, dosing every 12 hours.

Figure 4. Individual AUC_{0-24} of Midazolam, S-Warfarin, Dextromethorphan, and Caffeine, and Individual 6 hour Paraxanthine:Caffeine Ratios After Administration of a CYP Substrate Drug Cocktail Containing 0.2 mg Midazolam (CYP3A4), 10 mg Warfarin (CYP2C19), 30 mg Dextromethorphan (CYP2D6), and 100 mg Caffeine (CYP1A2) Either Alone, or In Combination with Abemaciclib After 7 Days of 200 mg Q12H Abemaciclib.

DMD Fast Forward. Published on June 24, 2020 as DOI: 10.1124/dmd.119.090092
This article has not been copyedited and formatted. The final version may differ from this version.

Individual data are denoted by open circles, individual change is denoted by dotted lines, and the geometric means of the individual data are denoted by filled circles.

AUC_{0-24}, area under the concentration versus time curve from zero to 24 hours; CYP, cytochrome P450; Q12H, dosing every 12 hours.

Figure 5. Forest Plot Showing the Change in AUC_{0-inf} and C_{max} of Midazolam, S-Warfarin, and Dextromethorphan, and the AUC_{0-12} and C_{max} of Caffeine, and the Paraxanthine:Caffeine AUC_{0-24} Ratio When Taken With or Without Abemaciclib (200 mg Q12H for 7 days) After a CYP Substrate Drug Cocktail Containing 0.2 mg Midazolam (CYP3A4), 10 mg Warfarin (CYP2C19), 30 mg Dextromethorphan (CYP2D6), and 100 mg Caffeine (CYP1A2).

AUC_{0-inf}, area under the concentration versus time curve from zero to infinity; AUC_{0-12}, area under the concentration versus time curve from zero to 12 hours; AUC_{0-24}, area under the concentration versus time curve from zero to 24 hours; C_{max}, maximal steady state plasma concentration; Dex, dextromethorphan; LSM, least square mean

DMD Fast Forward. Published on June 24, 2020 as DOI: 10.1124/dmd.119.090092
This article has not been copyedited and formatted. The final version may differ from this version.

Table 1. Demographics of Enrolled Patients

Parameter	Overall
Age, years, mean (SD)	60 (11)
Sex, n (%)	
Female	24 (54.5)
Male	20 (45.5)
Body mass index, kg/m^2, mean (SD)	28.5 (5.05)
Ethnicity, n (%)	
Hispanic or Latino	2 (4.5)
Not Hispanic or Latino	41 (92.2)
Unknown	1 (2.3)
Race, n (%)	
Asian	1 (2.3)
Black or African American	1 (2.3)
White	40 (90.9)
Unknown	2 (4.5)
ECOG status, %	
0	27.3
1	68.2
2	4.5

ECOG, Eastern Cooperative Oncology Group; SD, standard deviation

Table 2. PK Parameter Estimates of CYP Substrates

		Geometric Mean (CV%)			Ratio of Geometric LS Means (90% CI) Test:reference
Midazolam (0.2 mg)	**N**	**Midazolam**	**N**	**Midazolam + Abemaciclib**	
$AUC_{0\text{-}inf}$, ng*hr/mL	44	7.34 (74)	37	6.03 (63)	0.867 (0.775, 0.972)
C_{max}, ng/mL	44	2.12 (54)	37	1.75 (48)	0.845 (0.760, 0.940)
t_{max}, h[a]	44	0.50 (0.40-1.07)	37	0.50 (0.33-2.17)	0 (0, 0.0167)[b]
$t_{1/2}$, h	44	7.62 (2.23-31.20)	37	6.33 (3.27-13.00)	–
S-warfarin (10 mg)		Warfarin		Warfarin + Abemaciclib	
$AUC_{0\text{-}inf}$, ng*hr/mL	44	21400 (43)	30	20600 (40)	1.04 (0.956, 1.13)
C_{max}, ng/mL	44	561 (35)	30	526 (35)	0.935 (0.871, 1.00)
t_{max}, h[a]	44	1.01 (0.92-8.00)	30	1.02 (0.88-10.00)	0.00835 (0, 0.0666)[b]
$t_{1/2}$, h	44	43.0 (25.70-132.00)	30	42.2 (25.80-81.80)	–
Dextromethorphan (30 mg)		DEX		DEX + Abemaciclib	

$AUC_{0\text{-}inf}$, ng*hr/mL	42	32.6 (316)	35	32.1 (235)	0.976 (0.805, 1.18)
C_{max}, ng/mL	42	3.18 (182)	36	3.30 (164)	1.05 (0.898, 1.22)
t_{max}, h[a]	42	2.08 (0.93-6.00)	36	2.03 (1.07-10.25)	0 (0, 0.0500)[b]
$t_{1/2}$, h	42	10.90 (4.48-26.00)	35	9.44 (4.83-17.00)	–
Caffeine (100 mg)		Caffeine		Caffeine + Abemaciclib	
$AUC_{0\text{-}inf}$, ng*hr/mL	37	32500 (72)	30	47100 (89)	1.56 (1.35, 1.81)
C_{max}, ng/mL	39	2890 (29)	32	2950 (33)	1.01 (0.965, 1.06)
t_{max}, h[a]	39	0.52 (0.40-3.00)	32	0.53 (0.37-22.30)	0 (-0.0500, 0.250)
$t_{1/2}$, h	37	10.3 (2.96-35.50)	30	14.2 (4.43-51.20)	–
P:C $AUC_{0\text{-}24}$	30	0.452 (62)	26	0.345 (67)	0.683 (0.600, 0.777)
P:C 6 hour ratio	30	0.404 (76)	26	0.287 (79)	0.611 (0.516, 0.722)

[a]t_{max} is presented as median (min, max)

[b]ratio of t_{max} is presented as median of differences (90% CI)

$AUC_{0\text{-}inf}$, area under the concentration versus time curve from zero to infinity; $AUC_{0\text{-}24}$, area under the concentration versus time curve from zero to 24 hours; CI, confidence interval; C_{max}, maximal steady state plasma concentration; CV, coefficient of variation;

CYP, cytochrome P450; DEX, dextromethorphan; LS, least squares; P:C, paraxanthine to caffeine ratio; PK, pharmacokinetic; $t_{1/2}$, half-life; t_{max}, time of maximum observed drug concentration.

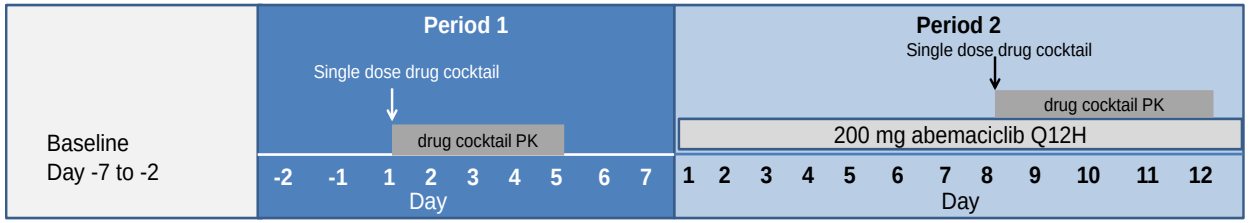

Figure 1.

DMD Fast Forward. Published on June 24, 2020 as DOI: 10.1124/dmd.119.090092
This article has not been copyedited and formatted. The final version may differ from this version.

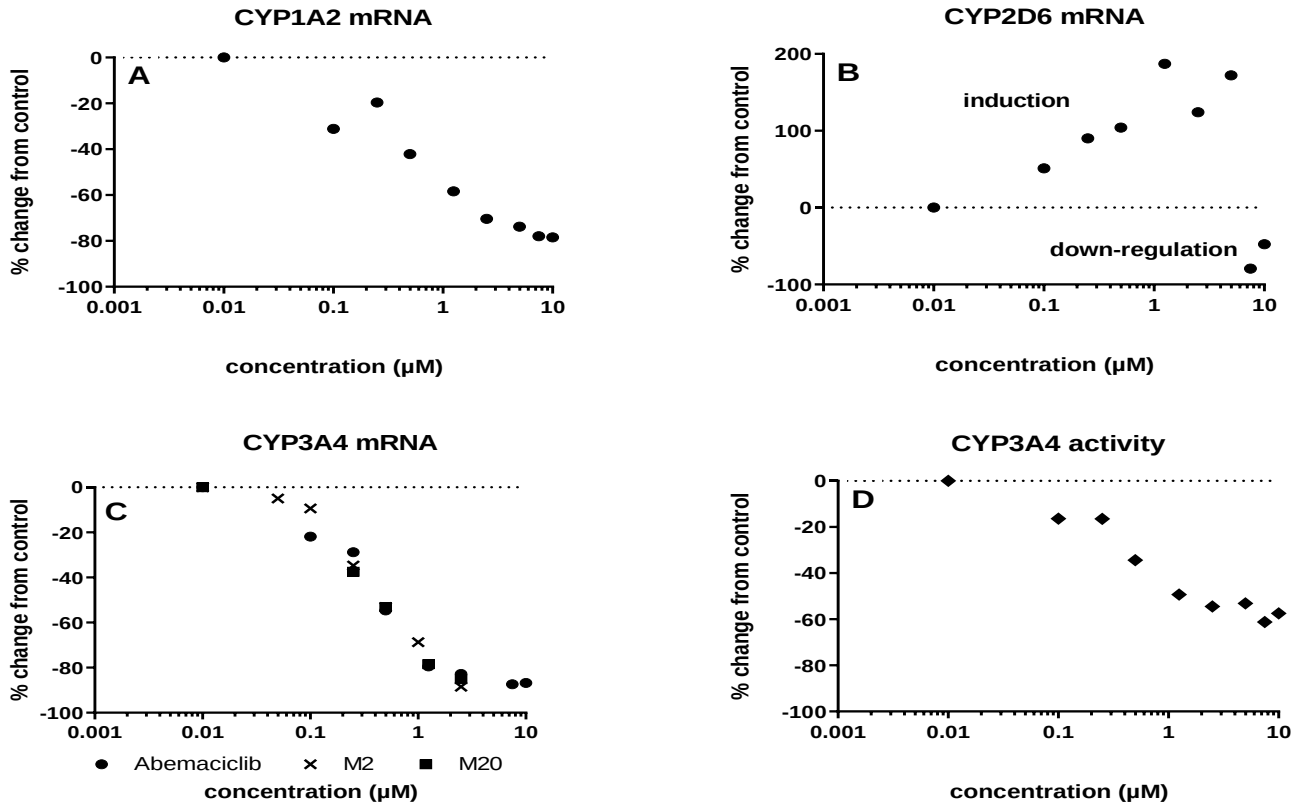

Figure 2.

DMD Fast Forward. Published on June 24, 2020 as DOI: 10.1124/dmd.119.090092
This article has not been copyedited and formatted. The final version may differ from this version.

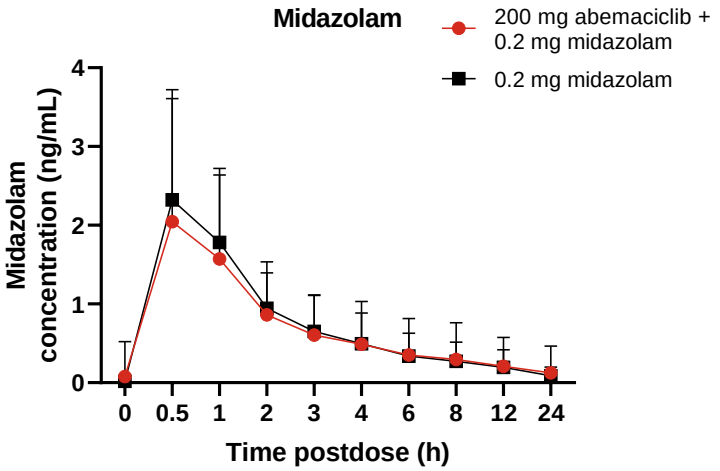

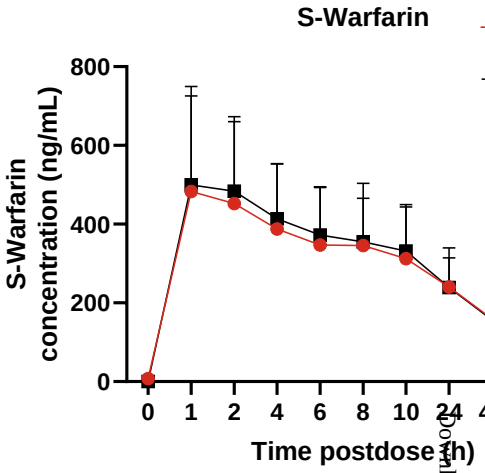

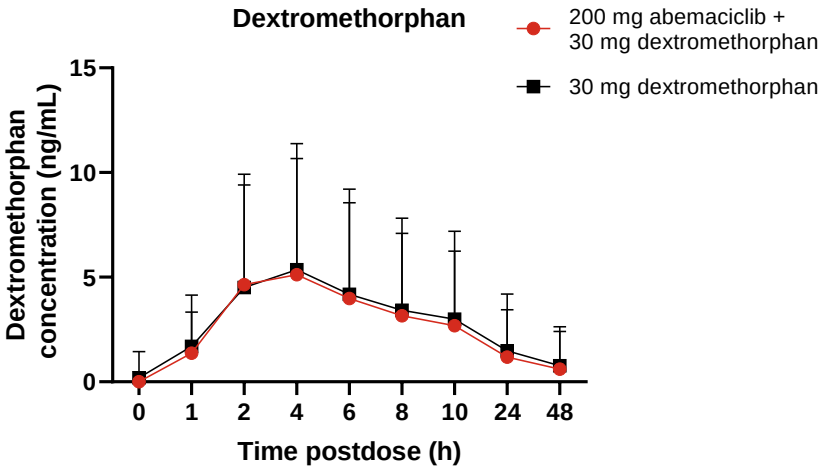

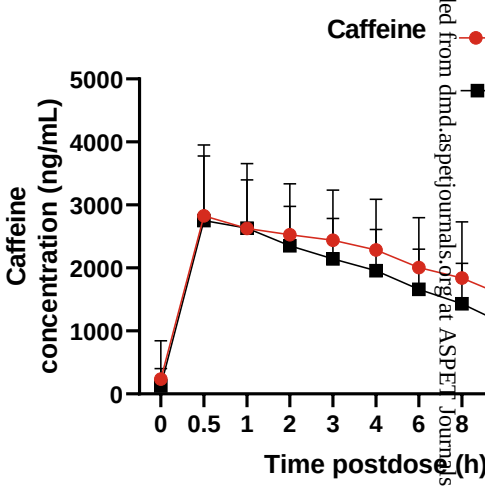

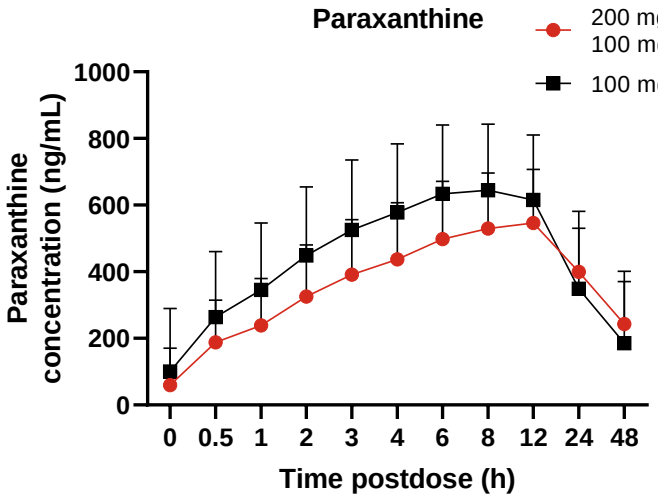

Figure 3.

DMD Fast Forward. Published on June 24, 2020 as DOI: 10.1124/dmd.119.090092
This article has not been copyedited and formatted. The final version may differ from this version.

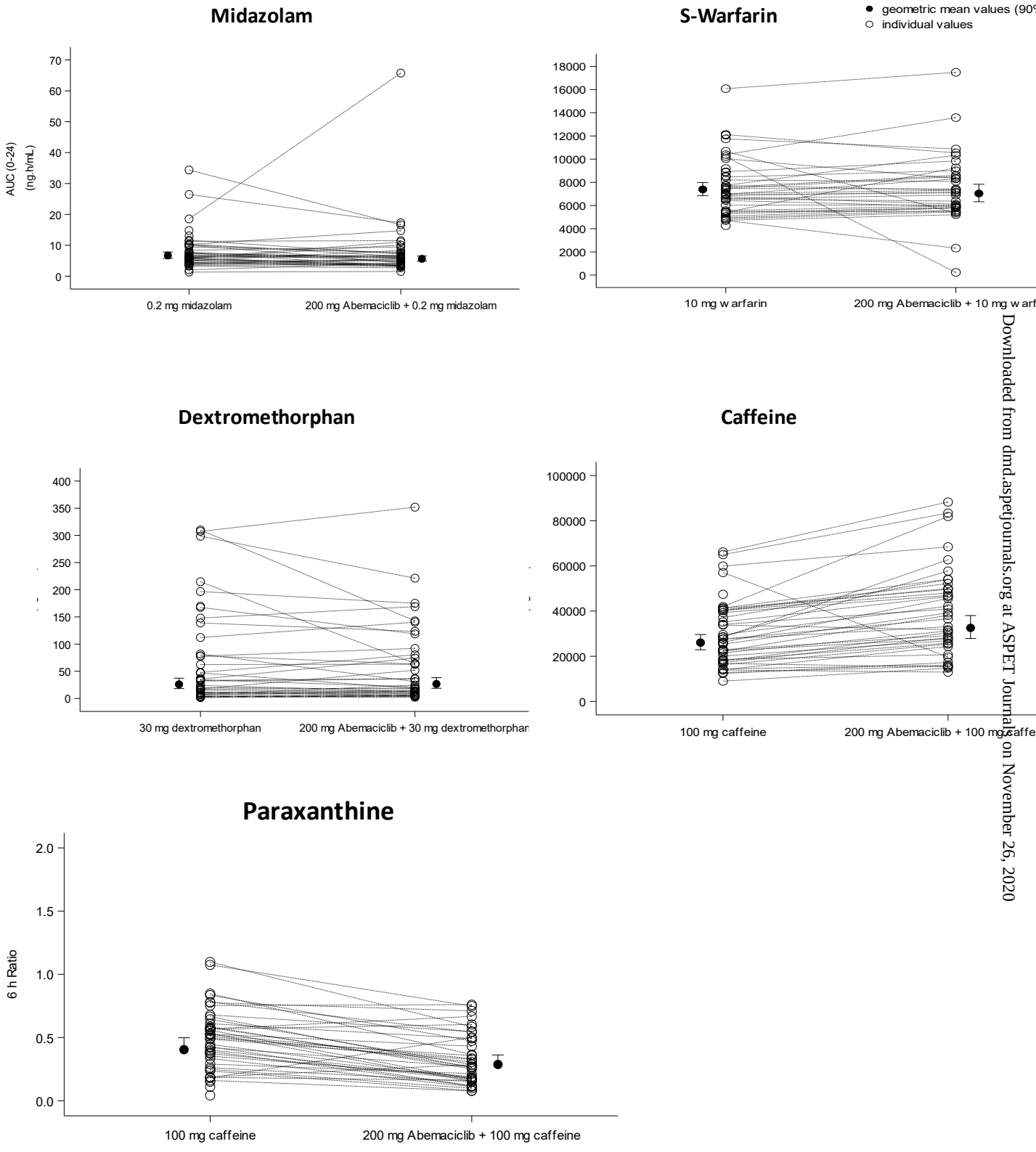

Figure 4.

DMD Fast Forward. Published on June 24, 2020 as DOI: 10.1124/dmd.119.090092
This article has not been copyedited and formatted. The final version may differ from this version.

DMD Fast Forward. Published on June 24, 2020 as DOI: 10.1124/dmd.119.090092
This article has not been copyedited and formatted. The final version may differ from this version.

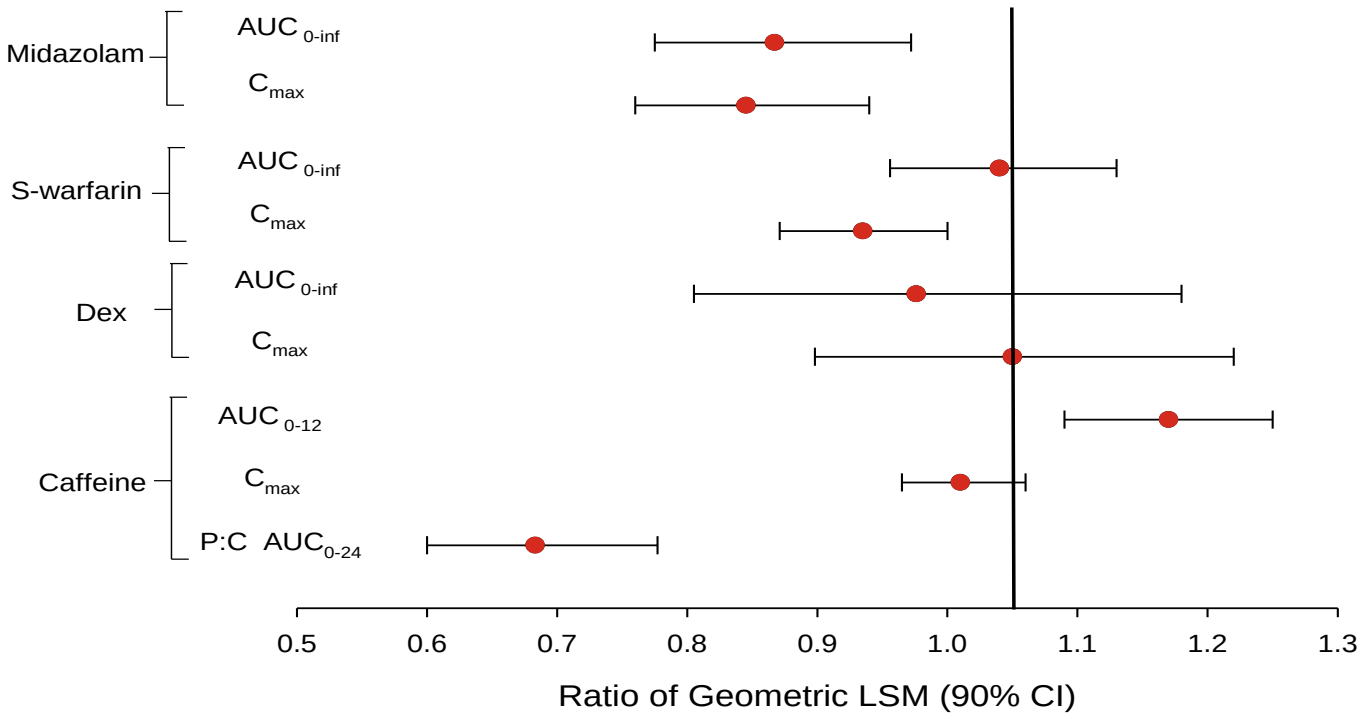

Figure 5.

Abemaciclib Does Not Have a Clinically Meaningful Effect on Pharmacokinetics of CYP1A2, CYP2C9, CYP2D6, and CYP3A4 Substrates in Patients with Cancer

P. Kellie Turner, Stephen D. Hall, Sonya C. Chapman, Jessica Rehmel,

Jane Royalty, Yingying Guo, Palaniappan Kulanthaivel

Drug Metabolism and Disposition Manuscript #90092

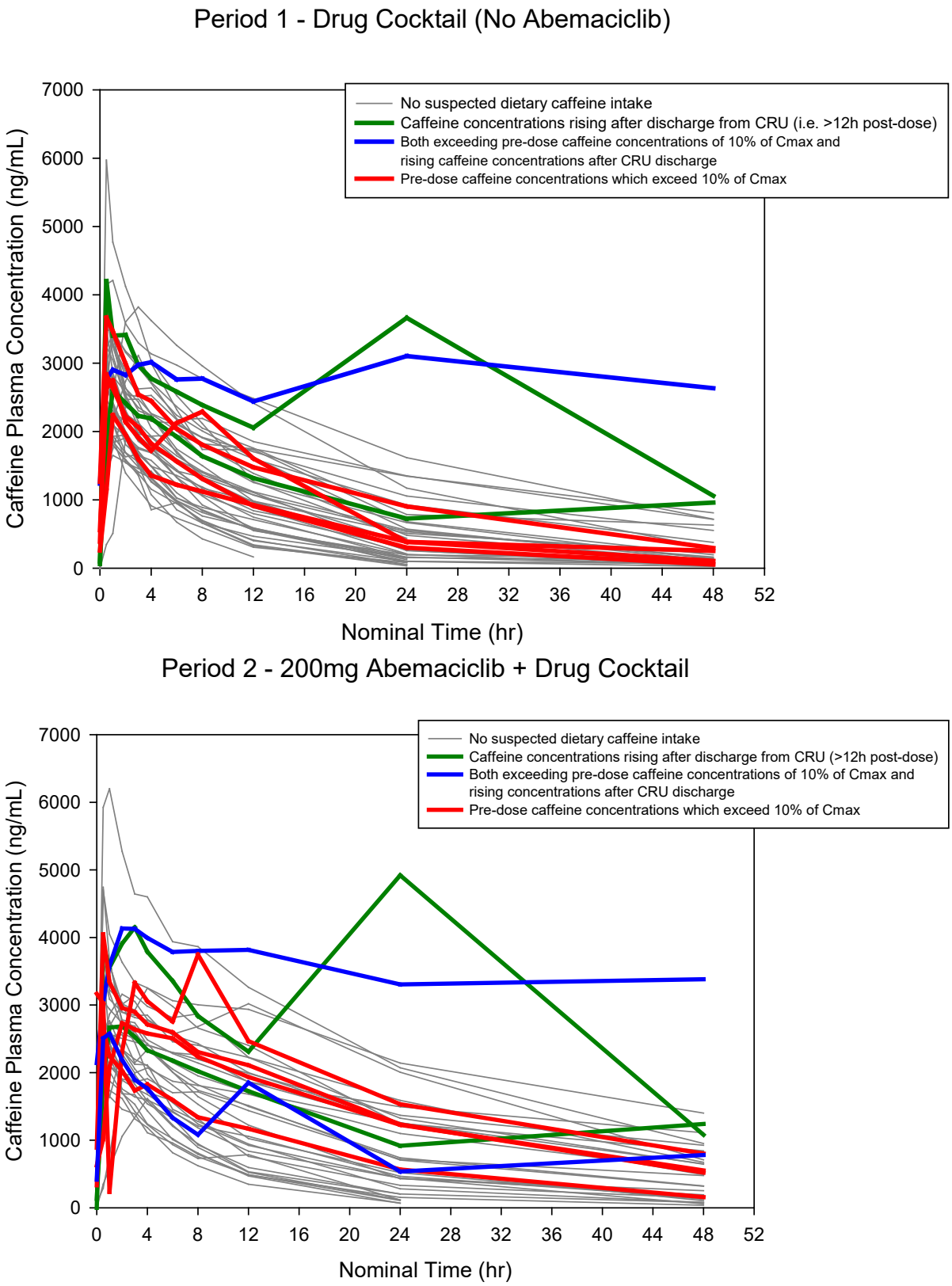

Supplemental Figure 1. Caffeine Plasma Concentrations in Individuals Who Appear to have Taken Dietary Caffeine in Period 1/2. Individual Plasma Concentration-Time Profiles

of Caffeine After Administration of a CYP Substrate Drug Cocktail Containing 0.2 mg Midazolam (CYP3A4), 10 mg Warfarin (CYP2C19), 30 mg Dextromethorphan (CYP2D6), and 100 mg Caffeine (CYP1A2) Either Alone (Period 1), or In Combination with Abemaciclib After 7 Days of 200 mg Q12H Abemaciclib (Period 2). Line colors denote patients who: have no suspected dietary caffeine intake (black); have concentrations which rise post-discharge from the CRU (>12h post- dose) (green); have pre-concentrations of caffeine which exceed 10% of post-dose C_{max} (red); or have both rising concentrations >12h post-dose and pre-dose concentrations of caffeine which exceed 10% of post-dose C_{max} (blue).

CRU, Clinical Research Unit; CYP, cytochrome P450; C_{max}, maximal steady state plasma concentration.

Supplemental Table 1. Selected details related to the conduct and interpretation of *in vitro* studies to assess the effects of abemaciclib, M2, and M20 on CYP mRNA and activity in cultured human hepatocytes, with selected E_{max} and EC_{50} values.

Test article	Abemaciclib	M2	M20
Hepatocytes (plated)	XenoTech Lot HC3-22; Caucasian female, age 57 years	XenoTech Lot HC10-1; Caucasian female, age 48 years XenoTech Lot HC3-22; Caucasian female, age 57 years XenoTech lot HC5-25; Caucasian male, age 56 years	XenoTech Lot HC10-1; Caucasian female, age 48 years XenoTech Lot HC3-22; Caucasian female, age 57 years XenoTech lot HC5-25; Caucasian male, age 56 years
[µM] tested for cytotoxicity by LDH release assay	Not tested in this study; used 0.1-10 µM (high conc. defined by prior study)	0.05-25 µM	0.1-10 µM
[µM] found cytotoxic initially	At 7.5 and 10 µM, some morphological changes but consistent with healthy cells	Morphological changes: 2.5-5 µM (moderate); 10-25 µM (severe)	Morphological changes: 2.5-5 µM (moderate); 10-25 µM (severe)
Description of initial cytotoxicity	# of vacuoles increased but cells remained cuboidal w/ intact membranes	2.5-5 µM: grainy cytoplasm 10-25 µM: grainy cytoplasm, LDH release, lysed membranes	2.5-5 µM: grainy cytoplasm 7.5-10 µM: grainy cytoplasm, LDH release, lysed membranes

Hepatocyte lot information	1 (prior study included 3 lots) XenoTech Catalog H1500.H15C+ Lot HC3-22	3 XenoTech Catalog H1500.H15C+ Lots HC10-1, HC3-22, and HC5-25	3 XenoTech Catalog H1500.H15C+ Lots HC10-1, HC3-22, and HC5-25
[µM] dosed for induction	0.1-10 µM	0.05, 0.1, 0.25, 0.5, 1, 2.5, 10, 25 µM	0.1, 0.25, 0.5, 1.25, 2.5, 5, 7.5, 10 µM
[µM] not reported due to cytotoxicity	none	10 and 25 µM	5, 7.5, and 10 µM
Description of later cytotoxicity	Not applicable	grainy cytoplasm, LDH release, lysed membranes, little/no enzyme activity, shifted GAPDH mRNA C_T values	grainy cytoplasm, LDH release, lysed membranes, little/no enzyme activity, shifted GAPDH mRNA C_T values
mRNA: induction of primary enzymes	1A2, 2B6, 3A4: no induction	1A2, 2B6, 3A4: no induction	1A2, 2B6, 3A4: no induction
mRNA: downregulation of primary enzymes (≥50% decrease)	1A2: decreases observed E_{max} -0.96-fold, EC_{50} 0.62 µM for HC3-22 2B6: decreases observed	1A2: decreases observed Unable to fit E_{max} and EC_{50} for HC10-1 2B6: decreases (2.5 uM only)	1A2: decreases observed E_{max} -0.63-fold, EC50 0.88 µM for HC10-1 2B6: decreases observed

	3A4: decreases observed E_{max} -0.89-fold, EC50 0.37 μM for HC3-22	3A4: decreases observed E_{max} -0.99-fold, EC50 0.44 μM for HC3-22 E_{max} -0.83-fold, EC50 0.25 μM for HC10-1 E_{max} -0.84-fold, EC50 1.3 μM for HC5-25	3A4: decreases observed E_{max} -0.82-fold, EC50 0.29 μM for HC3-22 E_{max} -1-fold, EC50 0.24 μM for HC10-1 (bottom fixed at -1)
mRNA: induction of secondary enzymes	2C8, 2C9, 2C19, 3A5: no induction 2D6: induction (1.25-5 μM; 2D6 generally not considered inducible); E_{max} 1.68-fold, EC50 0.21 μM for HC3-22	2C8, 2C9, 2C19, 2D6, 3A5: no induction	2C8, 2C9, 2C19, 2D6, 3A5: no induction
mRNA: downregulation of secondary enzymes (≥50% decrease)	2C8: no decreases 2C9: no decreases (44%; <50%) 2C19: no decreases 2D6: decreases (7.5-10 μM) 3A5: decreases observed	2C8: no decreases 2C9: decreases observed 2C19: no decreases 2D6: no decreases 3A5: no decreases	2C8: decreases observed 2C9: decreases observed 2C19: no decreases 2D6: no decreases 3A5: decreases observed

Activity: induction of primary enzymes	1A2, 2B6, 3A4: no induction	1A2, 2B6, 3A4: no induction	1A2, 2B6, 3A4: no induction
Activity: decreases (>50%) for primary enzymes	1A2: decreases observed 2B6: decreases observed 3A4: decreases observed	1A2: decreases (2.5 μM only) 2B6: decreases (2.5 μM only) 3A4: decreases (2.5 μM only)	1A2: decreases observed 2B6: decreases observed 3A4: decreases observed
Test article time-averaged % remaining (0-24 hrs; day 2)	27.5-48.6% remaining	37.0-58.5% remaining	39.3-71.5% remaining
Test article distribution (@24 hr; day 2)	1-16% in medium 84-99% in cell lysate	10-38% in medium 62-90% in cell lysate	5-27% in medium 73-95% in cell lysate

Conc, concentration; C_T, cycle threshold; EC_{50}, half maximal response concentration; E_{max}, maximum extent of induction or downregulation; GAPDH, glyceraldehyde 3-phosphate dehydrogenase; LDH, lactate dehydrogenase; M2, N-desethylabemaciclib; M20, hydroxyabemaciclib; mRNA, messenger ribonucleic acid. Where applicable, non-linear regression using a 4-parameter logistic model was used to estimate E_{max}, and EC_{50} (Graphpad Prism version 7, San Diego, CA).

Supplemental Table 2. TaqMan Gene Expression Assays used for RT-qPCR of mRNA isolated from human hepatocytes

Enzyme	Assay ID
GAPDH	Hs99999905_m1
CYP1A2	Hs00167927_m1
CYP2B6	Hs03044634_m1
CYP2C8	Hs00258314_m1
CYP2C9	Hs00426397_m1
CYP2C19	Hs00426380_m1
CYP2D6	Hs00164385_m1
CYP3A4	Hs00604506_m1
CYP3A5	Hs00241417_m1

ID, identification; mRNA, messenger ribonucleic acid; RT-qPCR, reverse transcription quantitative polymerase chain reaction.

Supplemental Table 3. Mass spectrometry conditions used for *in vitro* selective activity assays for CYP1A2, CYP2B6, and CYP3A from the *in vitro* study conducted in primary cultures of human hepatocytes

Enzyme	Substrate	Substrate Concentration (μM)[a]	Internal Standard	Incubation Time	Ionization Mode	Mass Transitions
CYP1A2	Phenacetin	100	Acetaminophen-d_4	45	ESI+	152.1/110.0
CYP2B6	Bupropion	500	Hydroxybuppropion-d_6	45	ESI+	256.1/238.0
CYP3A	Midazolam	30	1'-hydroxymidazolam-d_4	45	ESI+	342.0/323.9

[a]Bupropion and midazolam were co-incubated; equal volumes of supernatant from the phenacetin and bupropion/midazolam incubations were combined for analysis by LC/MS.

ESI, Electrospray ionization in the positive mode.

Supplemental Table 4. Parameters used as inputs for Equations 2 and 3

Parameter	Definition	Value	Source
$f_{u,p}$	Fraction of drug unbound in plasma	0.0557	Measured
C_{max}	Maximal steady-state plasma concentration	0.5 μM	Measured
F_a	Fraction absorbed	0.91	Estimated from human ^{14}C study (Kulanthaivel P et al. 2016)
k_a	Absorption rate constant	0.2 hr^{-1}	PopPK analysis (Tate SC, Sykes AK, Kulanthaivel P et al. 2018)
Dose	Highest approved dose	200 mg	Verzenio Prescribing Information (FDA)
Q_h	Hepatic blood flow	97 L/h	United States Food and Drug Administration 2017

R_b	Blood-to-plasma ratio	0.84	Measured
Q_{en}	Enterocyte blood flow	18 L/h	United States Food and Drug Administration 2017

C_{max}, maximal observed plasma concentration; F_a, fraction of drug absorbed; F_g, fraction of drug escaping metabolism in the gut; f_m, fraction of systemic clearance; $f_{u.p}$, fraction of drug unbound in plasma; k_a, absorption rate constant; R_b, blood-to-plasma ratio; Q_{en}, enterocyte blood flow**;** Q_h, hepatic blood flow.

Supplemental Table 5. Changes in CYP mRNA and activity measured in cultured hepatocytes following 2 days of treatment with abemaciclib, M2, and M20, presented as percent change from 0.1% DMSO control.

Concentration (uM)	0.05	0.1	0.25	0.50	1.0	1.25	2.5	5.0	7.5	10	25
Abemaciclib_CYP1A2_mRNA_HC3-22		-31	-20	-42		-58	-70	-74	-78	-79	
Abemaciclib_CYP1A2_Activity_HC3-22		-22	-23	-36		-46	-51	-53	-57	-55	
Abemaciclib_CYP2B6_mRNA_HC3-22		-14	-10	-37		-48	-57	-57	-47	-49	
Abemaciclib_CYP2B6_Activity_HC3-22		-23	-23	-42		-49	-55	-56	-66	-62	
Abemaciclib_CYP3A4_mRNA_HC3-22		-22	-29	-55		-80	-83		-87	-87	
Abemaciclib_CYP3A4_Activity_HC3-22		-16	-17	-34		-49	-55	-53	-61	-58	
Abemaciclib_CYP2C8_mRNA_HC3-22		-4	2	-5		-13	-8	6	16	20	
Abemaciclib_CYP2C9_mRNA_HC3-22		1	-8	-12		-32	-44	-39	-34	-33	
Abemaciclib_CYP2C19_mRNA_HC3-22		8	6	3		5	15	38	43	42	
Abemaciclib_CYP2D6_mRNA_HC3-22		51	90	104		187	124	172	-79	-48	
Abemaciclib_CYP3A5_mRNA_HC3-22		1	-4	-12		-25	-37	non-detect	-51	-44	
M2_CYP1A2_mRNA_HC10-1	-63	-61	-65	-71	-75		-91			cytotoxic	cytotoxic
M2_CYP1A2_mRNA_HC3-22	-7	-9	-39	-32	-46		-71			cytotoxic	cytotoxic
M2_CYP1A2_mRNA_HC5-25	15	23	37	30	43		17			cytotoxic	cytotoxic
M2_CYP2B6_mRNA_HC10-1	15	10	-7	-31	-49		-68			cytotoxic	cytotoxic
M2_CYP2B6_mRNA_HC3-22	-8	-6	-31	-35	-50		-58			cytotoxic	cytotoxic
M2_CYP2B6_mRNA_HC5-25	-5			-13	-25		-58			cytotoxic	cytotoxic
M2_CYP1A2_Activity_HC10-1	7	3	1	-7	-12		-50			cytotoxic	cytotoxic
M2_CYP1A2_Activity_HC3-22	-8	-13	-25	-25	-32		-45			cytotoxic	cytotoxic
M2_CYP1A2_Activity_HC5-25	-13	-17	-21	-27	-32		-47			cytotoxic	cytotoxic
M2_CYP2B6_Activity_HC10-1	25	14	9	-9	-19		-61			cytotoxic	cytotoxic
M2_CYP2B6_Activity_HC3-22	-11	-10	-26	-25	-36		-48			cytotoxic	cytotoxic
M2_CYP2B6_Activity_HC5-25	-12	-18	-26	-41	-45		-65			cytotoxic	cytotoxic
M2_CYP3A4_mRNA_HC10-1	30	-5	-35	-64	-72		-87			cytotoxic	cytotoxic
M2_CYP3A4_mRNA_HC3-22	-5	-9	-35	-53	-69		-89			cytotoxic	cytotoxic
M2_CYP3A4_mRNA_HC5-25	24	12	5	-14	-23		-57			cytotoxic	cytotoxic

M2_CYP3A4_Activity_HC10-1	21	9	3	-15	-24		-63			cytotoxic	cytotoxic
M2_CYP3A4_Activity_HC3-22	-7	3	-20	-26	-37		-51			cytotoxic	cytotoxic
M2_CYP3A4_Activity_HC5-25	-0.2	-10	-10	-26	-31		-44			cytotoxic	cytotoxic
M2_CYP2C8_mRNA_HC10-1	7	-1	-7	-20	-33		-46			cytotoxic	cytotoxic
M2_CYP2C8_mRNA_HC3-22	-16	-23	-24	-24	-27		-13			cytotoxic	cytotoxic
M2_CYP2C8_mRNA_HC5-25	-4	6	-7	-16	-20		-21			cytotoxic	cytotoxic
M2_CYP2C9_mRNA_HC10-1	17	-1	-4	-33	-53		non-detect			cytotoxic	cytotoxic
M2_CYP2C9_mRNA_HC3-22	14	11	6	-5	-17		-54			cytotoxic	cytotoxic
M2_CYP2C9_mRNA_HC5-25	13	1	1	-9	-8		-26			cytotoxic	cytotoxic
M2_CYP2C19_mRNA_HC10-1	-8	-17	-11	-9	-16		non-detect			cytotoxic	cytotoxic
M2_CYP2C19_mRNA_HC3-22	-6	-11	-8	-15	-12		-20			cytotoxic	cytotoxic
M2_CYP2C19_mRNA_HC5-25	18	7	16	7	9		10			cytotoxic	cytotoxic
M2_CYP2D6_mRNA_HC10-1	-15	-15	-11	-8	19		7			cytotoxic	cytotoxic
M2_CYP2D6_mRNA_HC3-22	6	2	4	2	13		-6			cytotoxic	cytotoxic
M2_CYP2D6_mRNA_HC5-25	7	7	28	28	48		34			cytotoxic	cytotoxic
M2_CYP3A5_mRNA_HC10-1	6	3	20	-7	-16		non-detect			cytotoxic	cytotoxic
M2_CYP3A5_mRNA_HC3-22	0	-6	-1	-21	-22		-26			cytotoxic	cytotoxic
M2_CYP3A5_mRNA_HC5-25	16	19	30	23	33		41			cytotoxic	cytotoxic
M20_CYP1A2_mRNA_HC10-1		-4	-21	-10		-56	-63	cytotoxic	cytotoxic	cytotoxic	
M20_CYP1A2_mRNA_HC3-22		39	10	-8		1	-28	cytotoxic	cytotoxic	cytotoxic	
M20_CYP1A2_mRNA_HC5-25		4	-10	6		22	41	cytotoxic	cytotoxic	cytotoxic	
M20_CYP2B6_mRNA_HC10-1		-14	-27	-23		-58	-51	cytotoxic	cytotoxic	cytotoxic	
M20_CYP2B6_mRNA_HC3-22		14	17	-1		-13	-22	cytotoxic	cytotoxic	cytotoxic	
M20_CYP2B6_mRNA_HC5-25		-7	-19	-25		-46	-58	cytotoxic	cytotoxic	cytotoxic	
M20_CYP3A4_mRNA_HC10-1		-30	-49	-65		-89	-90	cytotoxic	cytotoxic	cytotoxic	
M20_CYP3A4_mRNA_HC3-22		21	-38	-53		-79	-85	cytotoxic	cytotoxic	cytotoxic	

M20_CYP3A4_mRNA_HC5-25		0	-8	-8		-4	-42	cytotoxic	cytotoxic	cytotoxic	
M20_CYP1A2_Activity_HC10-1		-7	-14	-18		-39	-56	cytotoxic	cytotoxic	cytotoxic	
M20_CYP1A2_Activity_HC3-22		2	-10	-24		-28	-39	cytotoxic	cytotoxic	cytotoxic	
M20_CYP1A2_Activity_HC5-25		-12	-15	-22		-24	-34	cytotoxic	cytotoxic	cytotoxic	
M20_CYP2B6_Activity_HC10-1		-13	-24	-34		-53	-69	cytotoxic	cytotoxic	cytotoxic	
M20_CYP2B6_Activity_HC3-22		8	-37	-41		-49	non-detect	cytotoxic	cytotoxic	cytotoxic	
M20_CYP2B6_Activity_HC5-25		-16	-17	-39		-54	-66	cytotoxic	cytotoxic	cytotoxic	
M20_CYP3A4_Activity_HC10-1		-13	-20	-32		-56	-65	cytotoxic	cytotoxic	cytotoxic	
M20_CYP3A4_Activity_HC3-22		3	-17	-25		-38	-45	cytotoxic	cytotoxic	cytotoxic	
M20_CYP3A4_Activity_HC5-25		-12	-19	-20		-42	-49	cytotoxic	cytotoxic	cytotoxic	
M20_CYP2C8_mRNA_HC10-1		-23	-40	-25		-50	-32	cytotoxic	cytotoxic	cytotoxic	
M20_CYP2C8_mRNA_HC3-22		10	51	0		27	20	cytotoxic	cytotoxic	cytotoxic	
M20_CYP2C8_mRNA_HC5-25		-10	-29	-29		-50	-58	cytotoxic	cytotoxic	cytotoxic	
M20_CYP2C9_mRNA_HC10-1		-15	-35	-40		-67	-65	cytotoxic	cytotoxic	cytotoxic	
M20_CYP2C9_mRNA_HC3-22		-11	-10	-29		-43	-48	cytotoxic	cytotoxic	cytotoxic	
M20_CYP2C9_mRNA_HC5-25		12	-3	2		-4	-16	cytotoxic	cytotoxic	cytotoxic	
M20_CYP2C19_mRNA_HC10-1		-4	-15	-6		10	26	cytotoxic	cytotoxic	cytotoxic	
M20_CYP2C19_mRNA_HC3-22		4	0	13		14	11	cytotoxic	cytotoxic	cytotoxic	
M20_CYP2C19_mRNA_HC5-25		-2	-4	5		47	49	cytotoxic	cytotoxic	cytotoxic	
M20_CYP2D6_mRNA_HC10-1		7	-1	17		-10	2	cytotoxic	cytotoxic	cytotoxic	
M20_CYP2D6_mRNA_HC3-22		16	3	34		47	4	cytotoxic	cytotoxic	cytotoxic	
M20_CYP2D6_mRNA_HC5-25		6	12	26		41	39	cytotoxic	cytotoxic	cytotoxic	
M20_CYP3A5_mRNA_HC10-1		-9	-22	-20		-67	-70	cytotoxic	cytotoxic	cytotoxic	

M20_CYP3A5_mRNA_HC3-22		-11	-24	-31		-52	-61	cytotoxic	cytotoxic	cytotoxic	
M20_CYP3A5_mRNA_HC5-25		-4	4	11		8	39				

Cultured hepatocytes were incubated for 48 hours with abemaciclib, M2, and M20, at which time mRNA levels for CYP1A2, CYP2B6, CYP2C8, CYP2C9, CYP2C19, CYP2D6, CYP3A4, and CYP3A5 and CYP-selective activities for CYP1A2 (phenacetin O-deethylation to acetaminophen), CYP2B6 (bupropion hydroxylation), and CYP3A4 (midazolam 1'-hydroxylation) were measured. Values are presented as mean of 3 replicates. Blank cells = concentration not tested; non-detect = no amplification of mRNA; cytotoxic = concentration judged cytotoxic. Data are reported only for non-cytotoxic concentrations as determined by LDH release, increases in cycle threshold (CT) values for GAPDH, and/or morphological observations.